

Coordination of a Hemilabile N,N,S Donor Ligand in the Redox System $[\text{CuL}_2]^{+2+}$, $\text{L} = 2\text{-Pyridyl-}N\text{-(2'-alkylthiophenyl)methyleneimine}$

Johannes Schnödt,^[a] Jorge Manzur,^[b] Ana-Maria García,^[b] Ingo Hartenbach,^[a]
Cheng-Yong Su,^[c] Jan Fiedler,^[d] and Wolfgang Kaim^{*[a]}

Keywords: Copper / Diimines / Ligand effects / S ligands / Redox chemistry

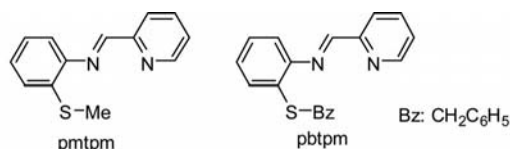
The new copper(I) complexes $[\text{Cu}(\text{L}^1)_2](\text{BF}_4)$, $\text{L}^1 = 2\text{-pyridyl-}N\text{-(2'-methylthiophenyl)methyleneimine}$, and $[\text{Cu}(\text{L}^2)_2](\text{ClO}_4)$, $\text{L}^2 = 2\text{-pyridyl-}N\text{-(2'-benzylthiophenyl)methyleneimine}$, have been prepared and structurally characterized. In contrast to the known $[\text{Cu}(\text{L}^1)_2](\text{ClO}_4)_2$, which exhibits partial thioether S binding to effect five-coordinate Cu^{2+} , the copper(I) compounds reported here contain four-coordinate metal ions with exclusively N-donor binding. Cyclic voltammetry reveals a fully reversible oxidation of the Cu^{I} species,

which suggests a small barrier for reorganization. The reduction at negative potentials is irreversible for compounds $[\text{Cu}(\text{L})_2](\text{X})$ and for the structurally characterized new compound $[\text{Cu}(\text{L}^1)(\text{PPh}_3)_2](\text{ClO}_4)$. UV/Vis spectroelectrochemistry shows the typical low-energy absorption bands of copper(I) (MLCT transition) and copper(II) (ligand-field transition) in the visible region; the Cu^{II} form develops an intense band at 350 nm attributed to a S-to-Cu ligand-to-metal charge transfer (LMCT).

Introduction

The strikingly different coordination properties of the neighbouring oxidation states Cu^{I} and Cu^{II} have provided a fruitful subject of investigation for electron transfer research, both within biochemistry (type 1 Cu of “blue” copper centres)^[1] and outside.^[2] The role of neutral thioether ligands mimicking the side chain of methionine has been studied for certain electron-transferring blue copper proteins and for recently characterized monooxygenase enzymes such as PHM (α -peptidylglycine hydroxylating monooxygenase)^[3,4] or D β M (dopamine- β -monooxygenase).^[4] In a more recent development, a copper(I) compound with a N_3S donor set including pyridine N and neutral S was found to react with CO_2 from air with oxidation to Cu^{2+} and formation of oxalate.^[5]

On the basis of a minimal model system involving copper(II) in combination with thioether-containing pyridyl-methyleneimines,^[6] we are now adding information on the copper(I) complex structures $[\text{CuL}_2]^+$, with ligands $\text{L} = \text{pmtpm}$ or pbtpm , and on the electrochemical and spectroelectrochemical aspects of the $\text{Cu}^{\text{I}}/\text{Cu}^{\text{II}}$ transition.



Results and Discussion

Copper(I) complexes $[\text{Cu}(\text{L}^1)_2](\text{BF}_4)$ and $[\text{Cu}(\text{L}^2)_2](\text{ClO}_4)$ were obtained by reacting the corresponding ligands with the precursor $[\text{Cu}(\text{CH}_3\text{CN})_4](\text{X})$, $\text{X} = \text{BF}_4^-$ or ClO_4^- , in the appropriate 2:1 molar ratio (Scheme 1). A 1:1 ratio between L^1 and $[\text{Cu}(\text{CH}_3\text{CN})_4](\text{ClO}_4)$ yielded $[\text{Cu}(\text{L}^1)(\text{CH}_3\text{CN})](\text{ClO}_4)$.

The structure determination of $[\text{Cu}^{\text{I}}(\text{L}^1)_2](\text{BF}_4)$ and $[\text{Cu}^{\text{I}}(\text{L}^2)_2](\text{ClO}_4)$ showed solely N-coordinated metal, in contrast to the corresponding copper(II) complex $[\text{Cu}(\text{L}^1)_2](\text{ClO}_4)_2$ with one coordinated thioether sulfur atom (Figures 1 and 2).

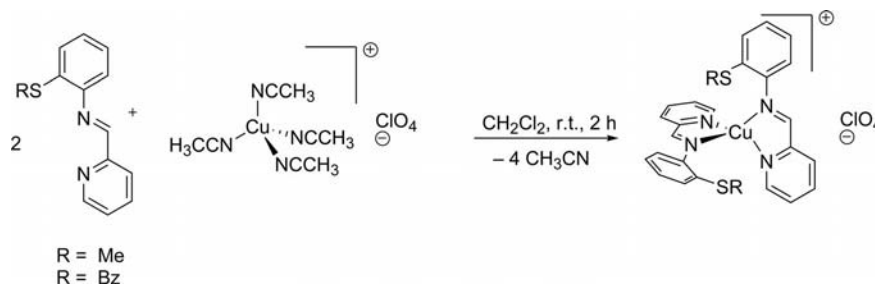
Bonding parameters are listed in Tables 1 and 2, crystal data are presented in Table 4. Within the bonding distance range of the metal, the difference between the nonbonding distances $\text{Cu}\cdots\text{S}$ 3.35 Å and the sole Cu–S bond of 2.43 Å in $[\text{Cu}(\text{L}^1)_2](\text{ClO}_4)_2$ are most conspicuous. This result clearly illustrates the coordination expansion on going from Cu^{I} (N_4 coordination) to Cu^{II} (N_4S coordination). In agreement with the typical Jahn–Teller distortion for d^9 systems, the latter was shown to exhibit a predominantly square-pyramidal configuration with an imine N at the apex (longest Cu–N bond to N2). Since the *mer* configuration is typically favoured over the *fac* form with unsaturated rigid tridentate ligands such as pyridine–Schiff base systems,^[7]

[a] Institut für Anorganische Chemie, Universität Stuttgart, Pfaffenwaldring 55, 70550 Stuttgart, Germany
E-mail: kaim@aic.uni-stuttgart.de

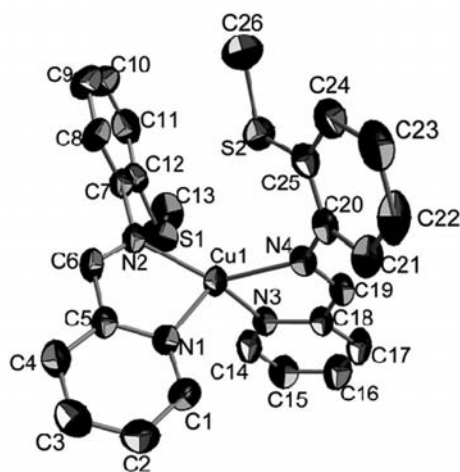
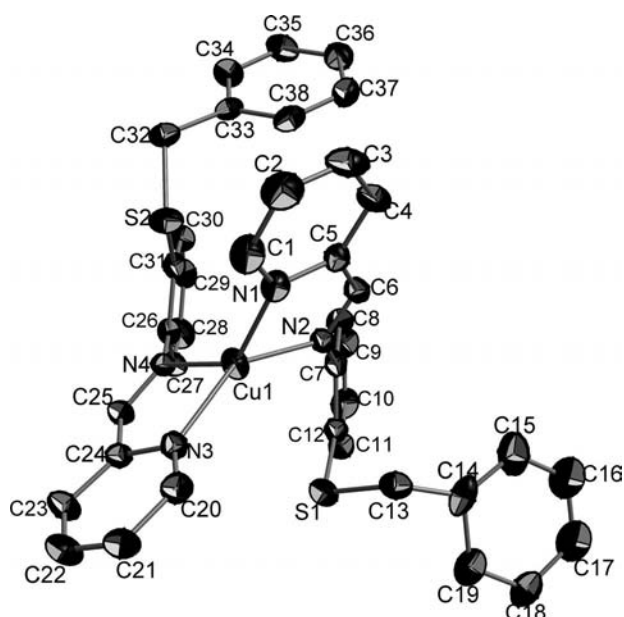
[b] Departamento de Ciencias de los Materiales, Facultad de Ciencias Físicas y Matemáticas, Universidad de Chile, Tupper 2069, Santiago de Chile, CEDENNA, Chile

[c] MOE Laboratory of Bioinorganic and Synthetic Chemistry, State Key Laboratory of Optoelectronic Materials and Technologies, School of Chemistry and Chemical Engineering, Sun Yat-Sen University, Guangzhou, 510275, China

[d] J. Heyrovský Institute of Physical Chemistry, v.v.i., Academy of Sciences of the Czech Republic, Dolejškova 3, 18223 Prague, Czech Republic



Scheme 1.

Figure 1. Molecular structure of $[\text{Cu}(\text{L}^1)_2]^+$ in the crystal of $[\text{Cu}(\text{L}^1)_2](\text{BF}_4)$, $\text{L}^1 = 2\text{-pyridyl-}N\text{-(2'-methylthiophenyl)methyleneimine}$.Figure 2. Molecular structure of $[\text{Cu}(\text{L}^2)_2]^+$ in the crystal of $[\text{Cu}(\text{L}^2)_2](\text{ClO}_4)$.

hexacoordination would imply *cis*-positioned thioether groups. In such a situation, the two weak Cu–S bonds cannot occupy the two apex sites of an elongated octahedron, leaving the square-pyramidal structure for the Cu^{II} com-

Table 1. Selected structure parameters for complexes $[\text{Cu}(\text{L}^1)_2](\text{BF}_4)$ and $[\text{Cu}(\text{L}^2)_2](\text{ClO}_4)$.^[a]

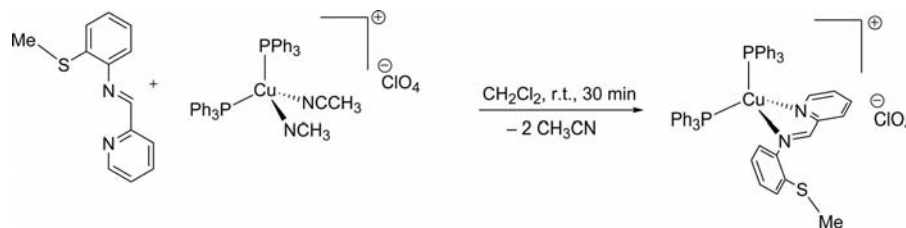
	$[\text{Cu}(\text{L}^1)_2](\text{BF}_4)$	$[\text{Cu}(\text{L}^2)_2](\text{ClO}_4)$	$[\text{Cu}(\text{L}^1)_2](\text{ClO}_4)_2$
Distances [Å]			
Cu–N1	2.079(3)	2.028(5)	1.954(5)
Cu–N2	2.035(2)	2.050(5)	2.153(6)
Cu–N3	2.030(3)	2.000(5)	2.007(5)
Cu–N4	2.104(2)	2.091(5)	1.952(5)
Cu–S1	3.402(1)	3.384(2)	3.699(3)
Cu–S2	3.405(2)	3.362(2)	2.431(2)
Angles [°]			
N1–Cu–N2	80.63(10)	80.6(2)	80.2(2)
N1–Cu–N3	116.28(11)	122.1(2)	100.7(2)
N1–Cu–N4	109.27(10)	134.55(2)	176.2(2)
N2–Cu–N3	136.20(11)	143.9(2)	117.0(2)
N2–Cu–N4	134.50(10)	103.42(2)	101.5(2)
N3–Cu–N4	80.51(10)	80.88(19)	81.5(2)
N1–Cu–S	–	–	95.92(17)
N2–Cu–S	–	–	97.49(15)
N3–Cu–S	–	–	143.61(18)
N4–Cu–S	–	–	80.57(16)

[a] N1,N3: pyridyl N; N2,N4: imine N.

plex. On the other hand, the two copper(I) ions $[\text{Cu}(\text{L}^1)_2]^+$ and $[\text{Cu}(\text{L}^2)_2]^+$ show quite irregular four-coordination, the former with a typical^[7,8] propensity towards a trigonal-pyramidal arrangement with a pyridine N (N1) at the apex (N1 is not involved in large N–Cu–N angles). The variation of the other Cu–N distances is marginal, with slightly longer bonds to the imine N atoms.

Table 2. Selected structure parameters for $[\text{Cu}(\text{L}^1)(\text{PPh}_3)_2](\text{BF}_4)$.

Distances [Å]	
Cu–N1	2.124(2)
Cu–N2	2.107(2)
Cu–P1	2.261(1)
Cu–P2	2.264(1)
Cu–S1	3.502(9)
Angles [°]	
N1–Cu–N2	78.43(9)
N1–Cu–P1	108.65(7)
N1–Cu–P2	112.74(7)
N2–Cu–P1	121.50(7)
N2–Cu–P2	103.83(6)
P1–Cu–P2	123.15(3)



Scheme 2.

Employing the copper(I) stabilizing effect of phosphane ligands, we also obtained compound $[\text{Cu}(\text{L}^1)(\text{PPh}_3)_2](\text{ClO}_4)$ by the standard route (Scheme 2) and determined its structure (Figure 3, Tables 2 and 4).

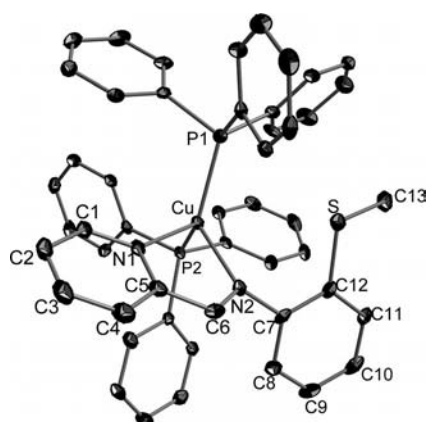


Figure 3. Molecular structure of $[\text{CuL}^1(\text{PPh}_3)_2]^+$ in the crystal of $[\text{CuL}^1(\text{PPh}_3)_2](\text{ClO}_4) \cdot \text{CH}_2\text{Cl}_2$.

The coordination around copper(I) is regular with a symmetrically binding N,N' -chelate system and two equivalent triphenylphosphane ligands. The asymmetry frequently noted in such $(N-N)\text{Cu}^{\text{I}}(\text{PR}_3)_2$ situations^[8] is not observed here.

Considering the structural change for $[\text{Cu}(\text{L}^1)_2]^+$ and $[\text{Cu}(\text{L}^1)_2]^{2+}$ ions as evident from solid-state structures, we investigated the electron transfer behaviour of the redox systems $[\text{CuL}_2]^{+/2+}$ by cyclic voltammetry at scan rates between 20 and 200 mVs^{-1} . A typical example is shown in Figure 4, and the results are summarized in Table 3. Standard reversible behaviour is observed under the conditions employed. A second oxidation, presumably of the coordinated thioether, occurs irreversibly at higher potentials.

These results suggest that the $\text{Cu}^{\text{I}}/\text{Cu}^{\text{II}}$ equilibrium depicted in Scheme 3 is attained very rapidly and requires only a small reorganization energy, in spite of the notable geometry change.

The potentials of the $\text{Cu}^{\text{I}}/\text{Cu}^{\text{II}}$ transition are not unusual; however, the reduction of the pyridylimino function to a radical anion^[9a,9b] occurs at rather negative values of about -1.6 V vs. $\text{Fc}^{+/0}$ and is not reversible, neither for $[\text{Cu}(\text{L})_2]^+$ nor for $[\text{Cu}(\text{L}^1)(\text{PPh}_3)_2]^+$. With more rigid and sterically better protected bis(α -diimine)copper complexes, for example those involving 2,9-disubstituted 1,10-phenanthroline,

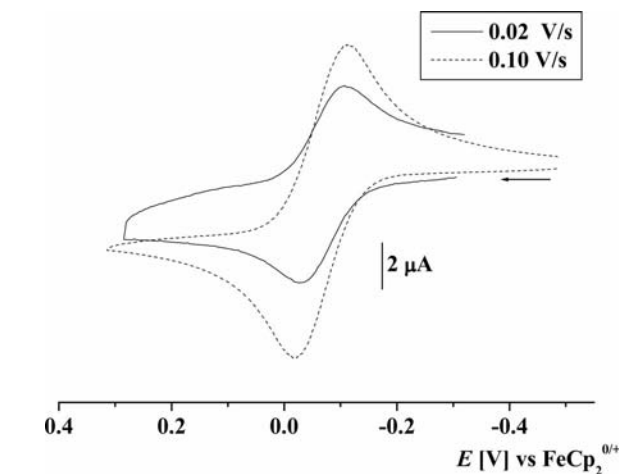
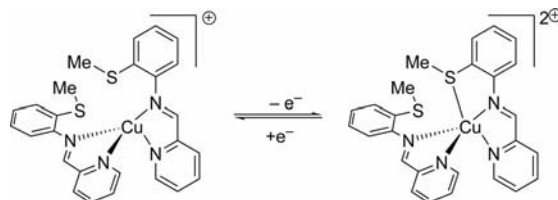


Figure 4. Cyclic voltammograms at different scan rates of $[\text{Cu}(\text{L}^1)_2](\text{BF}_4)$ in $\text{CH}_2\text{Cl}_2/0.1 \text{ M Bu}_4\text{NPF}_6$.

Table 3. Electrochemical data from cyclic voltammetry.^[a]

	$[\text{Cu}(\text{L}^1)_2](\text{BF}_4)$	$[\text{Cu}(\text{L}^2)_2](\text{ClO}_4)$	$[\text{Cu}(\text{L}^1)(\text{PPh}_3)_2](\text{ClO}_4)$
$E_{1/2}(\text{ox1})$	$-0.07^{[b]}$	$-0.08^{[c]}$	$+0.57 (E_{\text{pa}})^{[d]}$
$E_{\text{pa}}(\text{ox2})^{[d]}$	$+1.38$	-1.35	—
$E_{\text{pc}}(\text{red})^{[e]}$	-1.62	-1.63	-1.75

[a] In $\text{CH}_2\text{Cl}_2/0.1 \text{ M Bu}_4\text{NPF}_6$ at 100 mVs^{-1} scan rate; potentials in V vs. $\text{Fc}^{+/0}$. [b] At -45°C -0.09 V (reversible). [c] At -45°C -0.11 V (reversible). [d] E_{pa} : anodic peak potential for irreversible process. [e] E_{pc} : cathodic peak potential for irreversible process.



Scheme 3.

ines,^[9c] the reduced “copper(0)” states are more stable and can be correctly identified as radical ion complexes $[\text{Cu}^{\text{I}}(\text{L})(\text{L}^-)]$.

The seemingly clean reversibility of the $\text{Cu}^{\text{I}}/\text{Cu}^{\text{II}}$ transition prompted us to monitor this process for the $[\text{Cu}(\text{L}^1)_2]^+ / [\text{Cu}(\text{L}^1)_2]^{2+}$ system by UV/Vis spectroelectrochemistry (Figure 5).

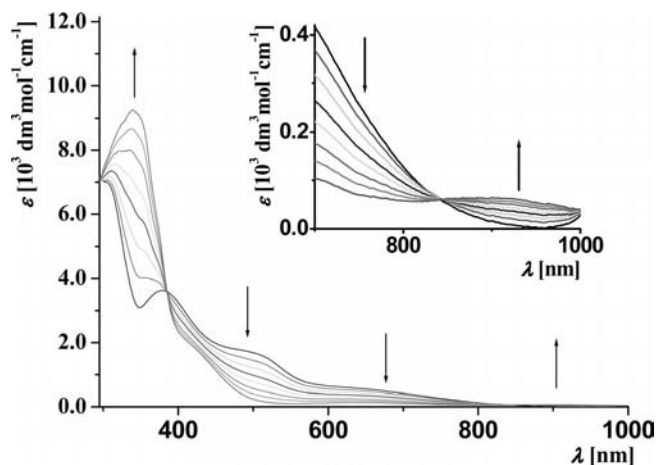


Figure 5. UV/Vis/NIR spectroelectrochemical oxidation of $[\text{Cu}(\text{L}^1)_2](\text{BF}_4)$ in $\text{CH}_2\text{Cl}_2/0.1 \text{ M Bu}_4\text{NPF}_6$.

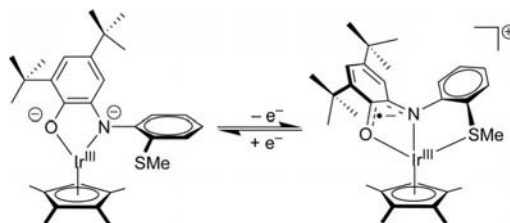
While the $[\text{Cu}^{\text{I}}(\text{L}^1)_2]^+$ ion exhibits the expected metal-to-ligand charge transfer (MLCT) absorptions in the visible region [650 nm (sh), 500 nm, (sh) 395 nm], which occur between the d^{10} level of copper(I) and the π^* orbitals of the iminopyridine conjugated π system, the oxidized form, $[\text{Cu}(\text{L}^1)_2]^{2+}$, has lost those absorptions but shows two new features: the expected very weak ligand–field (d–d) absorption around 900 nm and an intense new band at 355 nm, attributed to a sulfur-to-copper(II) ligand-to-metal charge transfer (LMCT). Since the sulfur is part of a neutral thioether function and not of a thiolate group,^[1] the LMCT transition occurs at high energy and the oxidized form displays the standard Cu^{II} EPR spectrum ($g_1 = 2.17$, $g_{2,3} = 2.02$, $A_1 = 15 \text{ mT}$).^[1]

Conclusions

The potentially tridentate ligand 2-pyridyl-*N*-(2'-methylthiophenyl)methyleneimine, which was previously reported to form a copper(II) complex ion $[\text{Cu}(\text{L}^1)_2]^{2+}$ with one *N,N'*- and one *N,N',S*-coordinating ligand L^1 , yielded a new copper(I) species, $[\text{Cu}(\text{L}^1)_2]^+$, with only *N*-coordinated ligands. Similarly, the structurally characterized analogue, $[\text{Cu}(\text{L}^2)_2]^+$, with the related ligand 2-pyridyl-*N*-(2'-benzylthiophenyl)methyleneimine (L^2) and the compound $[\text{Cu}(\text{L}^1)(\text{PPh}_3)_2](\text{ClO}_4)$ do not show any bonding between Cu^{I} and the thioether function ($\text{Cu}–\text{S}$ distances $> 3.35 \text{ \AA}$). The two described complex ions $[\text{CuL}_2]^+$ ($\text{L} = \text{L}^1, \text{L}^2$) exhibit differently distorted four-coordination at the d^{10} -configured metal. The transition $[\text{CuL}_2]^{+/2+}$ was monitored electrochemically by using cyclic voltammetry, EPR and UV/Vis spectroelectrochemistry, showing a fully reversible $\text{Cu}^{\text{I}}/\text{Cu}^{\text{II}}$ conversion despite the rather different molecular structures found in the crystals, that is, a distorted trigonal pyramid with pyridyl apex for $[\text{Cu}(\text{L}^1)_2]^+$ and a square pyramid with a thioether S atom at the apex for $[\text{Cu}(\text{L}^1)_2]^{2+}$. The spectroelectrochemical results are in agreement with the

oxidation state assignments. While the precursor solvate system $[\text{Cu}(\text{L}^1)(\text{CH}_3\text{CN})](\text{ClO}_4)$ is air-sensitive, the new copper(I) compounds do not react with O_2 .^[10]

It may be noted that the increase of the coordination number upon oxidation by thioether S binding is not only restricted to metal-centred electron removal as shown here but also via indirect effects from non-innocent ligand oxidation as exemplified recently in the system $[\text{Ir}(\text{Q})(\text{C}_5\text{Me}_5)]^{\text{ol}/+}$, $\text{Q} = 4,6\text{-di-}t\text{-butyl-(2-methylthiophenylimino)-}o\text{-benzoquinone}$, Scheme 4).^[11] In that case, however, the rearrangement involving a change in the metal coordination number leads to nonreversible behaviour in the cyclic voltammetric experiment, in contrast to the situation shown here.



Scheme 4.

Experimental Section

Instrumentation: EPR spectra in the X band were recorded with a Bruker System EMX. ^1H NMR spectra were taken with a Bruker AC 250 spectrometer. IR spectra were obtained with a Nicolet 6700 FTIR instrument; solid-state IR measurements were performed with an ATR unit (smart orbit with diamond crystal). UV/Vis/NIR absorption spectra were recorded with J&M TIDAS and Shimadzu UV 3101 PC spectrophotometers. Cyclic voltammetry was carried out in 0.1 M Bu_4NPF_6 solutions by using a three-electrode configuration (glassy carbon working, Pt counter and Ag/AgCl reference electrode) and a PAR 273 potentiostat and function generator. The ferrocene/ferrocenium (Fc/Fc^+) couple served as internal reference. Spectroelectrochemistry was performed with an optically transparent thin-layer electrode (OTTLE) cell. A two-electrode capillary served to generate intermediates for X band EPR studies.

$[\text{Cu}(\text{pmtpm})(\text{CH}_3\text{CN})](\text{ClO}_4)$: A solution of pmtpm (95 mg, 0.397 mmol)^[6] in dichloromethane (3 mL) was added to $[\text{Cu}(\text{CH}_3\text{CN})_4](\text{ClO}_4)$ (130 mg, 0.397 mmol) dissolved in dichloromethane (15 mL). The mixture turned red and was stirred for 1 h at room temperature. The complex was precipitated as a red brownish solid by reducing the amount of solvent in vacuo. For purification, the resulting powder was washed with toluene several times. Yield: 144 mg, 84.2%. $\text{C}_{15}\text{H}_{15}\text{ClCuN}_3\text{O}_4\text{S}$ (432.36): calcd. C 41.67, H 3.50, N 9.72; found C 41.94, H 3.64, N 9.42. ^1H NMR (400 MHz, CD_2Cl_2): $\delta = 2.19$ (s, 3 H, CH_3CN), 2.63 (s, 3 H, CH_3), 7.48 (s, 3 H, HPh, $\text{HC}=\text{N}$), 7.60–7.68 (m, 2 H, HPh), 8.03–8.10 (m, 2 H, HPy), 8.74 (s, 1 H, HPy), 8.83 (s, 1 H, HPy) ppm. ^{13}C -HSQC NMR (250 MHz, CD_2Cl_2): $\delta = 20.3$ (CH_3), 120.3 (CPh), 129.5 (CPh), 130.7 (CPy), 132.7 (CPy), 136.5 (CPy), 143.0 (CPh), 171.5 ($\text{C}=\text{N}$) ppm. HRMS: calcd. for $[\text{Cu}(\text{pmtpm})]^+$ ($\text{C}_{15}\text{H}_{12}\text{CuN}_2\text{S}$, $[\text{M}]^+$) 291.00; found 291.00.

$[\text{Cu}(\text{pmtpm})(\text{PPh}_3)_2](\text{ClO}_4)$: To $[\text{Cu}(\text{CH}_3\text{CN})_2(\text{PPh}_3)_2](\text{ClO}_4)$ (140 mg, 0.182 mmol) dissolved in dichloromethane (8 mL) was

added a yellow pmtpm solution (42 mg, 0.182 mmol) in dichloromethane (2.5 mL). After the mixture turned orange, it was stirred for another 30 min at room temperature. The amount of solvent was reduced in vacuo, and a brown solid precipitated after adding hexane. The solid was filtered off, and the orange solution was concentrated to dryness. For a further purification, the orange powder was washed five times with hexane (3 mL) and finally recrystallized from a dichloromethane solution. Yield: 33 mg, (0.033 mmol, 18.1%). $C_{49}H_{42}ClCuN_2O_4P_2S$ (915.88): calcd. C 64.26, H 4.62, N 3.06; found C 63.12, H 4.52, N 3.01. 1H NMR (250 MHz, CD_2Cl_2): δ = 1.86 (s, 3 H, CH_3), 6.39 (d, 3J = 7.6 Hz, 1 H, HPh), 6.98 (m, 1 H, HPh), 7.06 (t, 3J = 8.8 Hz, 12 H, CH), 7.19 (t, 3J = 7.5 Hz, 12 H, CH), 7.25–7.28 (m, 1 H, HPh), 7.30–7.33 (m, 1 H, HPh), 7.38 (t, 3J = 7.6 Hz, 6 H, CH), 7.48–7.54 (m, 1 H, HPy), 8.03–8.18 (m, 2 H, HPy), 8.27 (d, 3J = 4.7 Hz, 1 H, HPy), 8.57 (s, 1 H, HC=N) ppm. $^{31}P\{^1H\}$ NMR (250 MHz, CD_2Cl_2): δ = 1.00 ppm. HRMS: calcd. for $[Cu(pmtpm)(PPh_3)_2]^+$ ($C_{49}H_{42}CuN_2P_2S$, $[M]^+$) 815.18; found 815.18.

[Cu(pmtpm)₂](BF₄): To pmtpm (174 mg, 0.763 mmol) dissolved in dichloromethane (3 mL) was added dropwise a solution of $[Cu(CH_3CN)_4](BF_4)$ (120 mg, 0.382 mmol) in dichloromethane (11 mL). After being stirred at room temperature for 1.5 h, the deep red solution was concentrated in vacuo. The red solid, which precipitated after addition of toluene, was purified by recrystallization from a dichloromethane solution layered with toluene. Yield: 158 mg, (0.261 mmol, 68.4%). $C_{26}H_{24}BCuF_4N_4S_2$ (606.98): calcd. C 51.45, H 3.99, N 9.23; found C 51.39, H 4.03, N 9.24. 1H NMR (400 MHz, CD_2Cl_2): δ = 2.16 (s, 6 H, CH_3), 6.85 (d, 3J = 7.8 Hz, 2 H, HPh), 7.10 (t, 3J = 7.8 Hz, 2 H, HPh), 7.18–7.30 (m, 4 H, HPh), 7.70 (t, 3J = 5.0 Hz, 2 H, HPy), 7.93 (d, 3J = 7.7 Hz, 2 H, HPy), 8.1 (t, 3J = 7.7 Hz, 2 H, HPy), 8.57 (d, 3J = 4.7 Hz, 2 H, HPy), 8.64 (s, 2 H, HC=N) ppm. 1H - ^{13}C -HSQC NMR (250 MHz, CD_2Cl_2): δ = 15.6 (CH_3), 119.5 (CPh), 125.7 (CPh), 126.1 (CPh), 127.7 (CPy), 128.3 (CPy), 138.6 (CPy), 148.3 (CPy), 171.2 (CN) ppm. HRMS: calcd. for $[Cu(pmtpm)_2]^+$ ($C_{26}H_{24}CuN_4S_2$, $[M]^+$) 519.07; found 519.1.

[Cu(pbtpm)₂](ClO₄): A yellow solution of pbtpm (221 mg, 0.727 mmol) in dichloromethane (5 mL) was added to $[Cu(CH_3CN)_4](ClO_4)$ (119 mg, 0.364 mmol) dissolved in dichloromethane (13 mL). After the brown solution was stirred for 2 h at room temperature, the amount of solvent was reduced in order to precipitate the brown complex. For purification, the solid was recrystallized by dissolving in dichloromethane layered with toluene. Yield: 214 mg, (0.277 mmol, 76.1%). $C_{38}H_{32}ClCuN_4O_4S_2$ (771.81): calcd. C 59.13, H 4.18, N 7.26; found C 58.17, H 4.04, N 6.93. 1H NMR (250 MHz, CD_2Cl_2): δ = 3.84 (s, 4 H, CH_2), 6.73 (d, 3J = 7.7 Hz, 2 H, HPh), 6.92 (d, 3J = 7.6 Hz, 4 H, HPh), 7.04–7.23 (m, 10 H, HBz), 7.28 (d, 3J = 6.5 Hz, 2 H, HPh), 7.57 (t, 3J = 5.0 Hz, 2 H, HPy), 7.83 (d, 3J = 7.7 Hz, 2 H, HPy), 8.04 (t, 3J = 7.7 Hz, 2 H, HPy), 8.38 (s, 2 H, HC=N), 8.42 (d, 3J = 4.9 Hz, 2 H, HPy) ppm. 1H - ^{13}C -HSQC NMR (250 MHz, CD_2Cl_2): δ = 37.4 (CH_2), 120.5 (CPh), 128.6 (CPh), 126.6 (CBz), 126.7 (CPh), 128.3 (CPy), 128.0 (CPy), 138.3 (CPy), 148.4 (CPy), 170.4 (C=N) ppm. HRMS: calcd. for $[Cu(pbtpm)]^+$ ($C_{19}H_{16}CuN_2S$, $[M]^+$) 367.03; found 367.0.

X-ray Crystallography

Single crystals of the compounds were obtained by layering a solution in dichloromethane with toluene [for $Cu(L)_2$ complexes] or by cooling saturated solutions to $-10^\circ C$. Diffraction data were obtained by using Cu - K_α radiation (λ = 1.54178 Å) with an Oxford Gemini S Ultra diffractometer [for $Cu(L)_2$ complexes] or with Mo - K_α radiation (λ 0.71073 Å) with a Bruker Nonius Kappa-CCD instrument [for $[Cu(L)(PPh_3)_2](ClO_4)$]. The structures were solved with the SHELXS program (Patterson method) and refined with SHELXL97.^[12] All H atoms were introduced at the appropriate positions with isotropic temperature factors (Table 4).

CCDC-800172, -800173 and -800174 contain the supplementary crystallographic data for this paper. These data can be obtained free of charge from The Cambridge Crystallographic Data Centre via http://www.ccdc.cam.ac.uk/data_request/cif.

Table 4. Crystallographic data for the copper(I) complexes.

	$[Cu(L^1)_2](BF_4)$	$[Cu(L^2)_2](ClO_4)$	$[Cu(L^1)(PPh_3)_2](ClO_4) \cdot CH_2Cl_2$
Empirical formula	$C_{26}H_{24}BCuF_4N_4S_2$	$C_{38}H_{32}ClCuN_4O_4S_2$	$C_{50}H_{44}Cl_3CuN_4O_4P_2S$
Formula mass [g mol ⁻¹]	606.96	771.79	1000.76
Crystal system	Monoclinic	Monoclinic	Monoclinic
Space group	$C2/c$	$P2_1/n$	$P2_1/n$
<i>a</i> [Å]	27.984(2)	9.1487(3)	15.1636(4)
<i>b</i> [Å]	14.2186(7)	19.5317(7)	12.6726(3)
<i>c</i> [Å]	15.8971(12)	20.7615(7)	24.0858(6)
β [°]	117.466(10)	97.354(3)	98.404(2)
<i>V</i> [Å ³]	5612.3(7)	3679.3(2)	4578.7(2)
<i>Z</i>	8	4	4
<i>D</i> _{calcd} [g cm ⁻³]	1.437	1.393	1.452
<i>T</i> [K]	100(1)	100(1)	100(1)
λ [Å]	1.54178	1.54178	0.71073
θ range [°]	3.56–63.55	3.12–62.45	1.49–27.89
<i>F</i> (000)	2480	1592	2064
Parameters	343	532	745
μ [mm ⁻¹]	2.921	2.935	0.816
Refl. collected	21539	11551	20121
Indep. refl.	4582	5629	10897
Refl. [$I > 2\sigma(I)$]	3435	3421	7265
<i>R</i> ₁ / <i>wR</i> ₂ [all data]	0.0602/0.1654	0.1101/0.2032	0.0925/0.1318
<i>R</i> ₁ / <i>wR</i> ₂ [$I > 2\sigma(I)$]	0.0484/0.1566	0.0682/0.1834	0.0507/0.1180
Goodness of fit	1.055	1.024	1.054
$\Delta\rho$ [e Å ⁻³]	0.573/–0.417	0.551/–0.410	1.283/–1.035

Acknowledgments

Support from Deutsche Forschungsgemeinschaft (SFB 706), Fonds der Chemischen Industrie (Germany), COST D35 (European Union), Grant Agency of the Czech Republic (Grant 203/09/0705) and from Proyecto Basal CEDENNA-FB0807 (Chile) is gratefully acknowledged.

- [1] E. I. Solomon, M. A. Hanson in *Inorganic Electronic Structure and Spectroscopy, Vol. II* (Eds.: E. I. Solomon, A. B. P. Lever), Wiley, New York, **1999**, p. 1.
- [2] a) G. Chaka, J. L. Sonnenberg, H. B. Schlegel, M. J. Heeg, G. Jaeger, T. J. Nelson, L. A. Ochrymowycz, D. B. Rorabacher, *J. Am. Chem. Soc.* **2007**, *129*, 5217; b) E. A. Ambundo, Q. Yu, L. A. Ochrymowycz, D. B. Rorabacher, *Inorg. Chem.* **2003**, *42*, 5267; c) L. Zhou, D. Powell, K. M. Nicholas, *Inorg. Chem.* **2006**, *45*, 3840; d) L. Q. Hatcher, D.-H. Lee, M. A. Vance, A. E. Milligan, R. Sarangi, K. O. Hodgson, B. Hedman, E. I. Solomon, K. D. Karlin, *Inorg. Chem.* **2006**, *45*, 10055; e) N. W. Aboelella, B. F. Gherman, L. M. R. Hill, J. T. York, N. Holm, V. G. Young Jr., C. J. Cramer, W. B. Tolman, *J. Am. Chem. Soc.* **2006**, *128*, 3445; f) L. Zhou, K. M. Nicholas, *Inorg. Chem.* **2008**, *47*, 4356.
- [3] a) S. T. Prigge, B. A. Eipper, R. E. Mains, L. M. Amzel, *Science* **2004**, *304*, 864; b) J. P. Klinman, *J. Biol. Chem.* **2006**, *281*, 3013.
- [4] a) J. Klinman, *J. Biol. Chem.* **2006**, *281*, 3013; b) C. R. Hess, Z. Wu, A. Ng, E. E. Gray, M. A. McGuirl, J. P. Klinman, *J. Am. Chem. Soc.* **2008**, *130*, 11939; c) A. Kunishita, M. Kubo, H. Sugimoto, T. Ogura, K. Sato, T. Takui, S. Itoh, *J. Am. Chem. Soc.* **2009**, *131*, 2788.
- [5] R. Angamuthu, P. Byers, M. Lutz, A. L. Spek, E. Bouwman, *Science* **2010**, *327*, 313.
- [6] a) R. Balamurugan, M. Palaniandavar, H. Stoeckli-Evans, M. Neuburger, *Inorg. Chim. Acta* **2006**, *359*, 1103; see also b) A. Mangia, M. Nardelli, C. Pelizzi, G. Pelizzi, *J. Cryst. Mol. Struct.* **1971**, *1*, 139; c) M. Maji, M. Hossain, M. Chatterjee, S. K. Chattopadhyay, V. G. Puranik, P. Chakrabarti, S. Ghosh, *Polyhedron* **1999**, *18*, 3735; d) A. W. Addison, T. N. Rao, E. Sinn, *Inorg. Chem.* **1984**, *23*, 1957.
- [7] a) O. Rotthaus, V. Labet, C. Philouze, O. Jarjays, F. Thomas, *Eur. J. Inorg. Chem.* **2008**, 4215; b) S. Nayak, P. Gamez, B. Kozlevčar, A. Pevec, O. Roubeau, S. Dehnen, J. Reedijk, *Polyhedron* **2010**, *29*, 2291; c) C. Imbert, H. P. Hratchian, M. Lanznaster, M. J. Heeg, L. M. Hryhorczuk, B. R. McGarvey, H. B. Schlegel, C. N. Verani, *Inorg. Chem.* **2005**, *44*, 7414.
- [8] a) C. Vogler, W. Kaim, H.-D. Hausen, *Z. Naturforsch. Teil B* **1993**, *48*, 1470; b) M. Schwach, H.-D. Hausen, W. Kaim, *Chem. Eur. J.* **1996**, *2*, 446; c) M. Glöckle, K. Hübner, H.-J. Kümmerer, G. Denninger, W. Kaim, *Inorg. Chem.* **2001**, *40*, 2263; d) W. Kaim, J. Rall, *Angew. Chem.* **1996**, *108*, 47; *Angew. Chem. Int. Ed. Engl.* **1996**, *35*, 43.
- [9] a) A. Klein, V. Kasack, R. Reinhardt, T. Sixt, T. Scheiring, S. Zálíš, J. Fiedler, W. Kaim, *J. Chem. Soc., Dalton Trans.* **1999**, 575; b) M. van Gastel, C. C. Lu, K. Wieghardt, W. Lubitz, *Inorg. Chem.* **2009**, *48*, 2626; c) A. F. Stange, E. Waldhör, M. Moscherosch, W. Kaim, *Z. Naturforsch. Teil B* **1995**, *50*, 115.
- [10] a) E. Spodine, J. Manzur, *Coord. Chem. Rev.* **1992**, *119*, 171; b) P. Gamez, P. G. Aubel, W. L. Driessen, J. Reedijk, *Chem. Soc. Rev.* **2001**, *30*, 376; c) M. Merkel, N. Möller, M. Piacenza, S. Grimme, A. Rempel, B. Krebs, *Chem. Eur. J.* **2005**, *11*, 1201.
- [11] R. Hübner, S. Weber, S. Strobel, B. Sarkar, S. Zálíš, W. Kaim, *Organometallics*, accepted.
- [12] G. M. Sheldrick, *Acta Crystallogr., Sect. A* **2008**, *64*, 112.

Received: November 8, 2010

Published Online: February 18, 2011